

Small x behaviour of the chirally-odd parton distribution $h_1(x, Q^2)$

R. Kirschner¹, L. Mankiewicz^{2,*}, A. Schäfer³, L. Szymanowski^{3,★★}

¹Institut für Theoretische Physik und Naturwissenschaftlich-Theoretisches Zentrum, Universität Leipzig, Augustusplatz, D-04109 Leipzig, Germany

²Institut für Theoretische Physik, Technische Universität München, D-85747 München, Germany

³Institut für Theoretische Physik, J.W. Goethe Universität Frankfurt, Postfach 11 19 32, D-60054 Frankfurt, Germany

Received: 24 June 1996

Abstract. The small x behaviour of the structure function $h_1(x, Q^2)$ is studied within the leading logarithmic approximation of perturbative QCD. There are two contributions relevant at small x . The leading one behaves like $(1/x)^0$ i.e. it is just a constant in this limit. The second contribution, suppressed by one power of x , includes the terms summed by the GLAP equation. Thus for $h_1(x, Q^2)$ the GLAP asymptotics and Regge asymptotics are completely different, making $h_1(x, Q^2)$ quite an interesting quantity for the study of small x physics.

1 Introduction

The chirally-odd structure function $h_1(x, Q^2)$ appeared first in studies by Ralston and Soper [1] of the spin asymmetries in Drell-Yan processes (DY) for transversely polarized beams and targets. Its appearance is due to the fact that in DY processes the chiralities of quark lines originating in the same hadron are not correlated and amplitudes with different quark chiralities interfere. This is not possible for deep-inelastic scattering (DIS) where the chiralities of the quark lines have to be the same. The physical interpretation of $h_1(x, Q^2)$ structure function was given by Jaffe and Ji [2]: it measures the transversity asymmetry i.e. the difference of the probabilities to find a quark with spin polarized along the spin direction of a transversely polarized nucleon and respectively opposite to it.

Recently we are faced with the revival of interest in studies of polarized proton-nucleon collisions, both theoretically and experimentally. Several experiments at polarized hadronic colliders are planned for the near future.

The physical motivation for those experiments is reviewed in [3] and recently by Jaffe in [4]. In particular, the RHIC spin collaboration at BNL will provide in the near future a first measurement of $h_1(x, Q^2)$. Also the COMPASS collaboration at CERN plans to study this structure function.

The results of theoretical studies for $h_1(x, Q^2)$ are very limited so far. Because its decoupling from DIS this structure function was not an object of many investigations. A summary of results can be found in [5]. Below we would like to mention only some of the results which are relevant for the present work. The GLAP evolution equations for $h_1(x, Q^2)$ were studied by Artru and Mekhfi [6]. The anomalous dimensions corresponding to $h_1(x, Q^2)$ appeared already earlier in the Appendix of [7]. Collins has proved the factorization of hard and soft parts in DY processes, involving $h_1(x, Q^2)$ [8]. Recently Ioffe and Khodjamirian have calculated $h_1(x, Q^2)$ by means of the QCD sum rules [9].

The longitudinal spin effects and the transverse spin effects appear on equal footing in perturbative QCD. As both polarized structure functions $g_1(x, Q^2)$, measuring the helicity distribution and $h_1(x, Q^2)$, measuring the transversity distribution, contribute at the twist-two level to hard scattering processes, it is especially interesting to investigate their similarities and differences. In the non-relativistic limit these functions coincide but already in the bag model they are different [2].

We want to concentrate on the properties of polarized structure functions $g_1(x, Q^2)$ and $h_1(x, Q^2)$ in the kinematical region of small Björken variable x . While the small- x behaviour of $g_1(x, Q^2)$ is the subject of recent studies by Bartels et al. [10], we discuss in this paper the small- x behaviour of $h_1(x, Q^2)$.

Jaffe and Ji define $h_1(x, Q^2)$ as Fourier transform of the matrix element of the following bilocal quark operator on the light-cone [2]

$$h_1(x, Q^2) \mathcal{S}_{\perp\mu} = \frac{i}{2} \int_{-\infty}^{\infty} \frac{d\lambda}{2\pi} e^{i\lambda x} \langle p, \mathcal{S}_{\perp} | \bar{\psi}(0) \sigma_{\mu\nu} n^{\nu} \gamma_5 \psi(\lambda n) | p, \mathcal{S}_{\perp} \rangle, \quad (1.1)$$

Dedicated to Professor Wojciech Królikowski

*On leave of absence from N. Copernicus Astronomical Center, Polish Academy of Sciences, Warsaw, Poland

★★On leave of absence from Soltan Institute for Nuclear Studies, Warsaw, Poland

where $x = Q^2/2p \cdot q$, $Q^2 = -q^2$, n^μ is the light-cone vector, p^μ and \mathcal{S}_\perp^μ are the momentum and the transverse part of the spin vector $\mathcal{S} = (\mathcal{S} \cdot n)p + (\mathcal{S} \cdot p)n + \mathcal{S}_\perp$.

As was shown by Ioffe and Khodjamirian the structure function $h_1(x, Q^2)$ can also be related to a forward scattering matrix element between proton states of an operator containing an axial-vector and a scalar current [9]

$$\begin{aligned} T_\mu(p, q, \mathcal{S}_\perp) \\ = i \int d^4x e^{iqx} \langle p, \mathcal{S}_\perp | \frac{1}{2} T(j_{5\mu}(x)j(0) + j(x)j_{5\mu}(0)) | p, \mathcal{S}_\perp \rangle \\ = \tilde{h}_1(x, Q^2) \mathcal{S}_{\perp\mu} \end{aligned} \quad (1.2)$$

where $j_{5\mu}(x) = \bar{\psi}(x)\gamma_5\gamma_\mu\psi(x)$, $j(x) = \bar{\psi}(x)\psi(x)$ and in the second line of (1.2) only terms depending on the spin polarization vector \mathcal{S} are retained. Then, up to higher twist terms one gets

$$h_1(x, Q^2) = -\frac{1}{\pi} \text{Im} \tilde{h}_1(x, Q^2). \quad (1.3)$$

The perturbative contribution to $h_1(x, Q^2)$ involves the t -channel exchange of a quark and an antiquark of opposite chirality (parallel helicity). Amplitudes with such an exchange behave at large energy like s^0 plus logarithmic corrections [11]. This implies that for small x $h_1(x, Q^2)$ is roughly like $(1/x)^0$ i.e like a constant. On the other hand the one-loop parton splitting function is proportional to $x \approx Q^2/s$ at $x \rightarrow 0$. Therefore GLAP evolution [12] induces an asymptotics proportional to x , provided the input distribution has not a stronger asymptotics at $x \rightarrow 0$. The expectations from these simple arguments are confirmed by the following detailed analysis of the leading logarithm perturbative contributions.

The structure function $h_1(x, Q^2)$ contributes to the DY hadronic tensor ($p_A p_B \rightarrow \mu^+ \mu^- + X$) [2] as

$$\begin{aligned} W_{DY}^{\mu\nu} \sim [(\mathcal{S}_{A\perp} \cdot \mathcal{S}_{B\perp})(p_A^\mu p_B^\nu + p_A^\nu p_B^\mu - g^{\mu\nu} p_A \cdot p_B) \\ + (\mathcal{S}_{A\perp}^\mu \mathcal{S}_{B\perp}^\nu + \mathcal{S}_{A\perp}^\nu \mathcal{S}_{B\perp}^\mu) p_A \cdot p_B] \sum_q e_q^2 h_1^q(x) h_1^{\bar{q}}(y) \end{aligned} \quad (1.4)$$

where the sum runs over all quarks q and antiquarks \bar{q} . Because of the symmetry in $(\mu\nu)$ the signatures in the exchange channels to the hadron A and B are the same. Unlike in the case of g_1 in DIS, here both signatures $h_1^\pm = h_1^q \pm h_1^{\bar{q}}$ contribute. A definite signature contribution can be extracted by combining the data for DY production in proton-proton and proton-antiproton collisions.

The definition (1.2) leads to a positive signature amplitude. In [9] also another definition is mentioned, which leads to a negative signature amplitude. In the following we shall investigate the perturbative Regge asymptotics in the positive signature channel, starting from the formula (1.2).

In Sect. 2 we study the leading Regge asymptotics induced by the exchange of quark and antiquark. We rely on ideas related to the well known BFKL perturbative Pomeron [13] and the multi-Regge effective action [14]. The leading logarithm approximation applied here does

not include the coupling constant renormalization. The coupling constant in the formulas has to be considered as a fixed, determined by the typical transverse momentum scale.

In Sect. 3 we consider the double logarithmic contributions including the ones described by GLAP evolution at small x . Here we rely on the method of separation of soft particle [15] which has been applied recently in the studies of $g_1(x, Q^2)$ [10].

2 The leading log Regge asymptotics

2.1 Lowest order contribution

We calculate the lowest order contribution to $h_1(x, Q^2)$ first. For this purpose we adopt the parton model viewpoint and identify the proton with the on mass-shell quark. Thus the lowest order contribution to $T_\mu(p, q, \mathcal{S}_\perp)$ (1.2) is given by four graphs in Fig. 1. We obtain

$$T_\mu^{(0)}(p, q, \mathcal{S}_\perp) = \mathcal{S}_{\perp\mu} \left\{ \frac{s}{s - Q^2 + i\varepsilon} + \frac{-s}{-s - Q^2 + i\varepsilon} \right\} \quad (2.1)$$

where $s = 2p \cdot q$. The s -channel imaginary part of (2.1) leads to the usual lowest order result for the structure function in the parton model

$$h_1^{(0)}(x) = \delta(1 - x). \quad (2.2)$$

From (2.1) we learned that $h_1(x, Q^2)$ defined via (1.2) and (1.3) is related to positive signature exchange unlike $g_1(x, Q^2)$ which has negative signature [10]. The signature is relevant for the Regge asymptotics, i.e. the small x behaviour.

The leading log Regge asymptotics is calculated from graphs of the type Fig. 2. Those are the effective ladder diagrams in which the reggeized quarks of opposite chiralities propagate on both sides and interact through gluon exchange.

As a first step we consider the cut-vertex $\Phi^{(0)}$ coupling the exchanged fermions to the external currents (see Fig. 2)

$$\gamma_5 \gamma_\mu (\hat{k}_1 + \hat{q}) + (\hat{k}_1 + \hat{q}) \gamma_5 \gamma_\mu \quad (2.3)$$

where $\hat{k} = \gamma^\mu k_\mu$.

Only the transverse components of the currents are of interest, because of the projection with the transverse polarization vector $\mathcal{S}_{\perp\mu}$ (1.2). In the Regge asymptotics the contributions of the momentum k_1 are negligible.

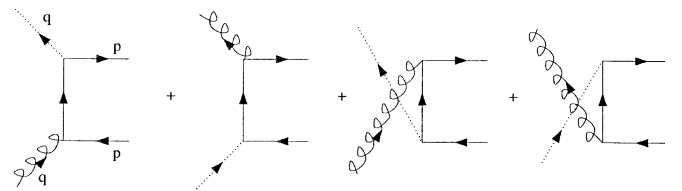


Fig. 1. Lowest order contribution to T_μ . The wavy line, the dotted line and the solid line denote the scattered axial meson, the scattered scalar and the exchanged quark, respectively

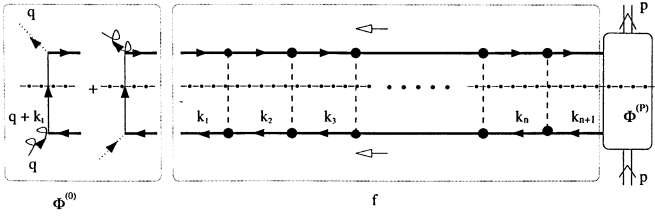


Fig. 2. The effective ladder diagram. The bold-solid line denotes the exchanged reggeized quark. The dashed line denotes produced gluon. The arrows on both sides of reggeized quarks emphasize that they have the same helicities (opposite chiralities). The bold dot denotes the effective vertex for gluon production. The dashed-dotted line emphasizes the calculations of s -channel discontinuity

It is convenient to adopt notations using light-cone components for the longitudinal parts and complex numbers for the transverse parts of all vectors, e.g.

$$k^\mu = \frac{2}{\sqrt{s}}(q_1^\mu k_- + p^\mu k_+) + k_\perp^\mu, \quad \kappa = k_\perp^1 + i k_\perp^2$$

$$q_1^\mu = q^\mu - \frac{q^2}{s} p^\mu. \quad (2.4)$$

We consider the following projectors for Dirac spinors

$$P_+ = -\frac{1}{4}\gamma\gamma^*, \quad P_- = -\frac{1}{4}\gamma^*\gamma, \quad \Pi_+ = \frac{1}{4}\gamma_-\gamma_+,$$

$$\Pi_- = \frac{1}{4}\gamma_+\gamma_-. \quad (2.5)$$

Notice that $\gamma_5 = i\gamma_0\gamma_1\gamma_2\gamma_3$ can be written as

$$\gamma_5 = (\Pi_+ - \Pi_-)(P_+ - P_-) \quad (2.6)$$

and that spinors in the subspaces $\Pi_- P_+$ and $\Pi_- P_-$ (or in subspaces $\Pi_+ P_-$ and $\Pi_+ P_+$) correspond to opposite chiralities.

For definiteness we consider below in this section that combination of amplitudes $T_\mu(p, s, \mathcal{S}_\perp)$ (1.2) which couples to external currents (2.3) with the matrix γ^*

$$T^*(p, s, \mathcal{S}_\perp) \equiv -(T_1(p, s, \mathcal{S}_\perp) - iT_2(p, s, \mathcal{S}_\perp))$$

$$= \mathcal{S}^* \tilde{h}_1(x, Q^2). \quad (2.7)$$

Thus with the notation (2.4) we have

$$\gamma_5 \gamma^* (\hat{k}_1 + \hat{q}) + (\hat{k}_1 + \hat{q}) \gamma_5 \gamma^* = q_- \gamma^* \gamma_+ + q_+ \gamma_- \gamma^*. \quad (2.8)$$

The second term can be omitted since q_+ is proportional to $x = Q^2/s$. We are left with the first term in (2.8) as the coupling of the external currents with the exchanged fermions.

2.2 Reggeon interaction

The leading logarithmic Regge asymptotics is determined by the exchange of a reggeized quark and antiquark of opposite chirality. A typical contribution is given by the graph in Fig. 2. The reggeons interact by gluon exchange. The gluons are coupled to the exchanged quarks by the effective vertex (3a), which includes besides the original

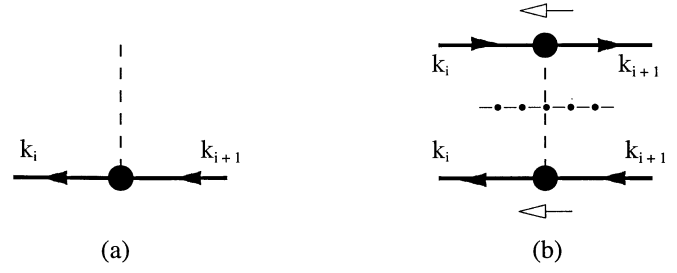


Fig. 3. The effective vertex for gluon production and the interaction kernel

QCD vertex contributions from bremsstrahlung production [17, 14]

$$\hat{V}^\mu(k_i, k_{i+1}) = \gamma_\perp^\mu - \frac{\hat{k}_{i\perp}}{k_i \cdot p} p^\mu - \frac{\hat{k}_{i+1\perp}}{k_{i+1} \cdot q_1} q_1^\mu. \quad (2.9)$$

In (2.9) the colour group generators are omitted since they play in the following a passive role.

The interaction kernel (Fig. 3b) is obtained by contracting two effective vertices assuming the exchanged gluon to be on mass-shell. We restrict ourselves to vanishing momentum transfer and we get

$$\hat{V}^\mu(k_i, k_{i+1}) \otimes \hat{V}_\mu(k_{i+1}, k_i)$$

$$= -\frac{1}{2}(\gamma \otimes \gamma^* + \gamma^* \otimes \gamma) \frac{|\kappa_i|^2 + |\kappa_{i+1}|^2}{|\kappa_i - \kappa_{i+1}|^2}$$

$$- \frac{1}{|\kappa_i - \kappa_{i+1}|^2} [\gamma^* \otimes \gamma^* \kappa_{i+1} \kappa_i + \gamma \otimes \gamma \kappa_{i+1}^* \kappa_i^*] \quad (2.10)$$

where \otimes indicates that the two γ -matrices are related to different fermionic lines in Fig. 3b. The first term on the rhs of (2.10) contributes to the exchange of quark and antiquark with equal chiralities. We are interested in the second term contributing to the opposite chirality exchange.

In Regge asymptotics the transverse part of the exchanged fermion propagator dominates i.e.

$$\frac{\hat{k}}{k^2} \rightarrow \frac{1}{2} \left(\gamma^* \frac{1}{\kappa^*} + \gamma \frac{1}{\kappa} \right). \quad (2.11)$$

A two particle amplitude $AB \rightarrow A'B'$ with a single fermion exchange of definite chirality $A_{1F}(s, q)$ has the Regge asymptotic form

$$A_{1F}(s, q) = \Phi_{A'A}(q) \frac{s^{\alpha_F(q)}}{q} \Phi_{B'B}(q) \quad (2.12)$$

where here and in the formulas below of this subsection q is the (transverse part of the) momentum transfer vector in the complex number notation. The functions $\Phi_{A'A}(s, q)$ and $\Phi_{B'B}(s, q)$ are the impact factors describing the coupling of the Regge pole to the scattered particles.

The Regge trajectory $\alpha_F(q)$ is given by

$$\alpha_F(q) = \frac{g^2 C_F}{(2\pi)^3} \bar{\alpha}_F(q), \quad C_F = \frac{N^2 - 1}{2N},$$

$$\bar{\alpha}_F(q) = - \int \frac{d^2 \kappa}{|q - \kappa|^2} \cdot \frac{q}{\kappa}, \quad (2.13)$$

N being the number of colours. Some intermediate regularization is needed to define the integral. It can be omitted from the resulting equation (2.18) due to the cancellation of infrared divergencies.

The Regge asymptotics of scattering amplitudes is represented in terms of partial waves $\mathcal{A}^\pm(\omega, q)$

$$A(s, q) = A^+(s, q) + A^-(s, q)$$

$$A^\pm(s, q) = \int_{-i\infty}^{i\infty} \frac{d\omega}{2\pi i} \zeta^\pm(\omega) \left(\frac{s}{\mu^2} \right)^\omega \mathcal{A}^\pm(\omega, q) \quad (2.14)$$

where $A^+(s, q)$ ($A^-(s, q)$) is the crossing even (odd) part of the amplitude $A(s, q)$ and $\zeta^\pm(\omega)$ is the signature factor. For the leading behaviour of the amplitude $T_\mu(p, q, \mathcal{S}_\perp)$ related to $h_1(x, Q^2)$ (see (1.2) and (1.3)) only small values of ω are important. Then in the case of positive signature the signature factor can be omitted, $\zeta^+(\omega) \approx 1$.

The partial wave describing the sum of the graphs in Fig. 2 has the form

$$\mathcal{A}^+(\omega, q) = \int d^2 \kappa \frac{d^2 \bar{\kappa}}{\bar{\kappa}^2} \Phi^{(0)}(\kappa, q) \cdot f(\omega, \kappa, \bar{\kappa}, q) \cdot \Phi^{(P)}(\bar{\kappa}, q). \quad (2.15)$$

The impact factor $\Phi^{(0)}(\kappa, q)$ describes the coupling to the external currents (see (2.8)) and the impact factor $\Phi^{(P)}(\bar{\kappa}, q)$ describes the coupling of the scattered proton to the exchanged reggeons. $f(\omega, \kappa, \bar{\kappa}, q)$ is the two-reggeon Green function for which we would like to formulate now the equation describing the sum of graphs in Fig. 2.

Writing the partial wave for the one-fermion exchange amplitude (2.12) we see that reggeized fermion exchange corresponds to the propagator

$$\frac{1}{\omega - \alpha_F(q)} \cdot \frac{\gamma}{q} + \frac{1}{\omega - \alpha_F^*(q)} \cdot \frac{\gamma^*}{q^*}. \quad (2.16)$$

The two-fermion exchange of opposite chirality is represented by

$$\frac{1}{\omega - \alpha_F(\kappa) - \alpha_F(\kappa - q)} \cdot \frac{\gamma}{\kappa} \otimes \frac{\gamma}{\kappa - q}$$

$$+ \frac{1}{\omega - \alpha_F^*(\kappa) - \alpha_F^*(\kappa - q)} \cdot \frac{\gamma^*}{\kappa^*} \otimes \frac{\gamma^*}{\kappa^* - q^*}. \quad (2.17)$$

Now we have all building blocks (2.10), (2.17) for the equation describing the interacting two-fermion exchange. Choosing the component in the reggeon-current coupling proportional to $\gamma^* \gamma_+$ (2.8) (so the impact factor $\Phi^{(0)}(\kappa, 0)$ is just 1) we pick up the corresponding terms from the propagators (2.17) and the interaction kernel (2.10). The resulting expression (proportional to $\gamma \gamma_+$) implies that the

reggeon Green function $f(\omega, \kappa, \bar{\kappa})$ at $q = 0$ is the solution of the equation

$$[\omega - 2\alpha_F(\kappa)] f(\omega, \kappa, \bar{\kappa})$$

$$= \delta^{(2)}(\kappa - \bar{\kappa}) + \frac{g^2 C_F}{(2\pi)^3} \int d^2 \kappa' \frac{2}{|\kappa - \kappa'|^2} \cdot \frac{\kappa'}{\kappa} \cdot f(\omega, \kappa', \bar{\kappa}). \quad (2.18)$$

This equation is the analogon of the BFKL Pomeron equation [13] for the case of opposite chirality fermion exchange. It has been considered together with the equation for equal chirality fermion exchange in [18].

The solution of equation (2.18) can be written in terms of the eigenfunctions $\phi_{n,v}(\kappa)$

$$\phi_{n,v}(\kappa) = |\kappa|^{2iv} \left(\frac{\kappa}{|\kappa|} \right)^{1+n} \quad (2.19)$$

and eigenvalues $(g^2 C_F / 8\pi^2) \Omega(n, v)$

$$\Omega(n, v) = 4\psi(1) - \psi\left(\frac{1}{2} + iv + \frac{n}{2}\right) - \psi\left(\frac{1}{2} - iv + \frac{n}{2}\right)$$

$$- \psi\left(\frac{1}{2} + iv - \frac{n}{2}\right) - \psi\left(\frac{1}{2} - iv - \frac{n}{2}\right) \quad (2.20)$$

of the homogeneous equation. We obtain

$$f(\omega, \kappa, \bar{\kappa}) = \frac{1}{2\pi^2} \cdot \frac{1}{\kappa^2} \sum_{n=-\infty}^{\infty} \int_{-\infty}^{\infty} dv \cdot \frac{\phi_{n,v}(\kappa) \cdot \phi_{n,v}^*(\bar{\kappa}) \cdot \left(\frac{\bar{\kappa}}{\bar{\kappa}^*} \right)}{\omega - (g^2 C_F / 8\pi^2) \Omega(n, v)}. \quad (2.21)$$

After convolution with the impact factor $\Phi^{(0)}(\kappa, 0) = 1$ (see (2.15)) only the term with $n = 1$ contributes. The Regge singularity appears at the value ω_1 , where the two poles in v from the denominator in (2.21) pinch the integration contour

$$\omega_1 = \frac{g^2 C_F}{8\pi^2} \Omega(1, 0) = 0. \quad (2.22)$$

Notice that for the singularity ω_0 of the contribution $n = 0$ we have $\omega_0 = (g^2 / \pi^2) C_F \ln 2 > \omega_1$. The decoupling due to the structure of $\Phi^{(0)}(\kappa, 0)$ prevents the $n = 0$ contribution from dominating the asymptotics. This decoupling of the right-most singularity is a special feature of the considered exchange channel.

2.3 Coupling to the proton

The impact factor $\Phi^{(P)}(\bar{\kappa})$ carries the non-trivial information about the proton structure which we are not able to calculate from perturbative QCD. We adopt the following form for this impact factor

$$\Phi^{(P)}(\kappa) = \frac{\hat{p}}{\sqrt{s}} (\mathcal{S}_\perp k_\perp) \hat{k}_\perp \gamma_5 \mathcal{F}^{(P)}(|\kappa|^2). \quad (2.23)$$

The function $\mathcal{F}^{(P)}(|\kappa|^2)$ can be a Gaussian with a width determined by the scale of the proton mass.

With the ansatz (2.23) we are able to calculate the partial wave $\mathcal{A}^+(\omega, 0)$ from (2.15). The inverse of Mellin transform (2.14) gives the discontinuity of the scattering amplitude

$$\text{Disc } T^*(p, q, \mathcal{S}_\perp) = -i\mathcal{S}^* \frac{1}{\sqrt{\pi\Omega_0 \ln(1/x)}} \int \frac{Q^2 d^2\kappa}{|\kappa|^2} \cdot \int d^2\bar{\kappa} \exp\left(-\frac{\ln^2(|\kappa|^2/|\bar{\kappa}|^2)}{4\Omega_0 \ln(1/x)}\right) \cdot \mathcal{F}^{(P)}(|\bar{\kappa}|^2) \quad (2.24)$$

where

$$\Omega_0 = \frac{g^2 C_F}{2\pi^2} \zeta(3). \quad (2.25)$$

The integral over κ can be expressed in terms of the incomplete gamma function $\Phi(x)$ [19]. We finally obtain the following expression for the leading small x asymptotics of the structure function $h_1(x, Q^2)$

$$h_1(x, Q^2)|_{\text{Regge}} = \frac{1}{2} \int d^2\bar{\kappa} \left(1 + \Phi\left(\frac{\ln(Q^2/|\bar{\kappa}|^2)}{\sqrt{4\Omega_0 \ln(1/x)}}\right)\right) \cdot \mathcal{F}^{(P)}(|\bar{\kappa}|^2). \quad (2.26)$$

Equations (2.21), (2.22) and (2.26) are our main results.

3 Summing double-logarithmic contributions

3.1 The GLAP evolution of $h_1(x, Q^2)$

The contributions summed up above have been extracted in the leading $\ln s$ approximation, i.e. only the contribution of each loop with a logarithmic longitudinal momentum integral has been taken into account. Now we consider the contributions with a logarithm from the transverse momentum part of each loop integral. It turns out that the longitudinal momentum integral in these contributions can also be approximated in some region by a logarithm. Our aim is to sum up the resulting double log contributions.

We start with the one loop graphs shown in Fig. 4 which contribute to the s -channel discontinuity and we choose the axial gauge $A_\mu q_1^\mu = 0$

$$\text{Disc } T_\mu^{(1)}(p, q, \mathcal{S}_\perp) = \frac{i}{2} g^2 C_F \int \frac{d^4 k}{(2\pi)^4} \frac{\mathcal{N}_\mu^{\rho\sigma} \cdot d_{\rho\sigma}(p-k)}{(k^2 + i\epsilon)^2} \cdot (-2\pi i)^2 \delta_+[(p-k)^2] \delta_+[(k+q)^2] \quad (3.1)$$

where $d_{\rho\sigma}(k)$ is the nominator of the axial gauge gluonic propagator and $\mathcal{N}_\mu^{\rho\sigma}$ is the matrix element related to a quark line

$$d_{\rho\sigma}(k) = g_{\rho\sigma} - \frac{q_{1\rho} k_\sigma + k_\rho q_{1\sigma}}{q_1 \cdot k} \\ \mathcal{N}_\mu^{\rho\sigma} = \bar{u}(p, \mathcal{S}_\perp) \gamma^\rho \hat{k} [\gamma_5 \gamma_\mu (\hat{k} + \hat{q}) + (\hat{k} + \hat{q}) \gamma_5 \gamma_\mu] \cdot \hat{k} \gamma^\sigma u(p, \mathcal{S}_\perp). \quad (3.2)$$

We restrict ourselves to vanishing momentum transfer. The scattering quark with momentum p is assumed to be

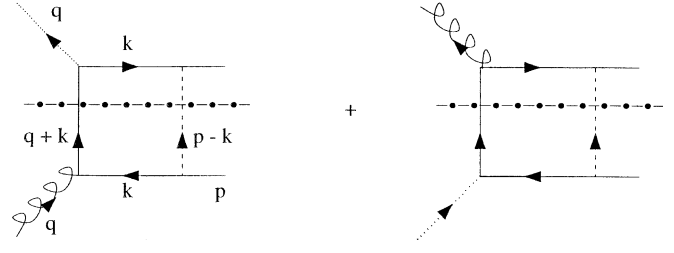


Fig. 4. The one-loop contribution to T_μ

on mass-shell and we project out the contribution proportional to the transverse polarization vector \mathcal{S}_\perp as in Sect. 2.1

$$\mathcal{N}_\mu^{\rho\sigma} d_{\rho\sigma}(p-k) = -\frac{4sk^2}{q_1 \cdot (p-k)} \cdot [2\mathcal{S}_{\perp\mu}(q_1 k) + k^2 \mathcal{S}_{\perp\mu} - k_\mu (\mathcal{S}_\perp k)]. \quad (3.3)$$

We parametrize the loop momentum k as $k = \alpha q_1 + \beta p + k_\perp$ and we use the complex number notation (2.4). The contribution with a logarithmic κ integral arises from the first term in the square bracket of (3.3)

$$\text{Disc } T_\mu^{(1)}(p, q, \mathcal{S}_\perp) = \mathcal{S}_{\perp\mu} \frac{(-i)g^2 C_F}{2\pi} \int d\alpha d\beta \frac{d|\kappa|^2}{|\kappa|^2} \cdot \frac{\beta}{1-\beta} \delta_+ \left[\beta - x - \frac{|\kappa|^2}{s} \cdot \frac{1-x}{1-\beta} \right] \cdot \delta_+ \left[\alpha + \frac{|\kappa|^2}{s(1-\beta)} \right] \\ \approx \mathcal{S}_{\perp\mu} \frac{(-i)g^2 C_F}{2\pi} \cdot \frac{x}{1-x} \int \frac{d|\kappa|^2}{|\kappa|^2}. \quad (3.4)$$

As a contribution to deep-inelastic scattering the κ integral results into $\ln Q^2$ and the coefficient is to be identified (see (1.3)) as the parton (GLAP) splitting function (before regularizing the singularity at $1-x$ appropriately)

$$P^{(0)}(x) = 2C_F \frac{x}{1-x} \quad (3.5)$$

We recover the known one-loop result for the splitting function [6] respectively the resulting anomalous dimensions [7]

We compare the result (3.4) from the viewpoint of Regge asymptotics with the one obtained in Sect. 2. The contribution (3.4) is down by one power of s compared to the ones analysed in (2.26). From this we learn that for $h_1(x, Q^2)$ the small x asymptotics of the GLAP evolution does not reproduce the leading perturbative Regge behaviour.

3.2 Double-logs in higher orders

Now we analyse how the contributions with a logarithmic κ integral emerge in higher loops. In particular we are

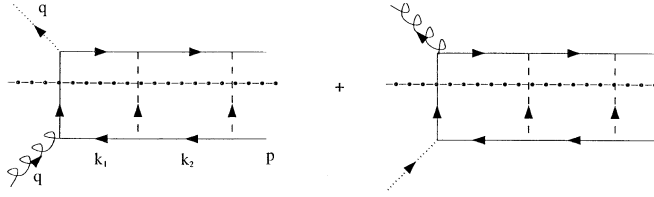


Fig. 5. The two-loop contribution to T_μ

interested in the integration region resulting in a logarithmic contribution from each transverse momentum loop integral.

The GLAP equation, describing the large Q^2 behaviour of structure functions, sums the leading log contributions of the considered type only for strongly ordered transverse momenta. We shall see that in our case this is not the only region which gives leading logarithms from the transverse momentum integrals.

We analyse the two-loop integral from Fig. 5. We extract from the numerator, consisting of the Dirac trace and the factors $d_{\mu\nu}$ of the gluons propagators, the contributions proportional to $k_1^2 \cdot k_2^2$ resulting in the leading logarithms. We obtain

$$\begin{aligned} \text{Disc } T_\mu^{(2)}(p, q, \mathcal{S}_\perp) &= \mathcal{S}_{\perp\mu} \frac{(-i)g^4 s^3}{(2\pi)^5} \int d\alpha_1 d\alpha_2 d\beta_1 d\beta_2 \frac{d^2\kappa_1}{s\alpha_1\beta_1 - |\kappa_1|^2} \\ &\cdot \frac{d^2\kappa_2}{s\alpha_2\beta_2 - |\kappa_2|^2} \cdot P^{(0)}(\beta_2) P^{(0)}\left(\frac{\beta_1}{\beta_2}\right) \\ &\cdot \delta_+ [s(1 + \alpha_1)(\beta_1 - x) - |\kappa_1|^2] \cdot \delta_+ [s(\alpha_1 - \alpha_2) \\ &\cdot (\beta_1 - \beta_2) - |\kappa_1 - \kappa_2|^2] \\ &\cdot \delta_+ [s\alpha_2(\beta_2 - 1) - |\kappa_2|^2] . \end{aligned} \quad (3.6)$$

We perform the integration over α_1 and α_2 and obtain that both κ integrals are logarithmic in the region

$$\begin{aligned} 1 \gg \beta_2 \gg \beta_1 \gg \frac{\mu^2}{s} \\ |\kappa_2^2| < |\kappa_1^2| \frac{\beta_2}{\beta_1} \end{aligned} \quad (3.7)$$

(μ^2 is the infrared cut-off). This is the integration range encountered in the leading double-log asymptotics of equal chirality fermion exchange [20]. Because of this analogy it is not necessary to go beyond two-loops. We are able to write down the integral equation summing up all contributions logarithmic in both the κ and β integrals.

It is convenient to write the equation for the sum of ladders without the external currents as denoted in Fig. 2 by f (there f refers to the partial wave, the corresponding amplitude will be denoted by $A(\beta, |\kappa^2|)$)

$$\begin{aligned} A(\beta_1, |\kappa_1^2|) &= \frac{g^2}{2(2\pi)^2} \int_{\beta_1}^1 \frac{d\beta_2}{\beta_2} \int_{\mu^2}^{|\kappa_1^2|\beta_2/\beta_1} \frac{d|\kappa_2^2|}{|\kappa_2^2|} P^{(0)}\left(\frac{\beta_1}{\beta_2}\right) A(\beta_2, |\kappa_2^2|) \\ &+ A_0(\beta_1, |\kappa_1^2|) \\ A_0(\beta_1, |\kappa_1^2|) &= \frac{g^2}{2(2\pi)^2} P^{(0)}(\beta_1) . \end{aligned} \quad (3.8)$$

The structure function $h_1(x, Q^2)$ in the small x region ($\mu^2 \ll Q^2 \ll s$) is obtained from $A(\beta_1, |\kappa_1^2|)$ by

$$h_1(x, Q^2) = \int_{\mu^2/s}^1 \int_{\mu^2}^{s/4} \frac{d|\kappa_1^2|}{|\kappa_1^2|} \delta\left[\beta_1 - x - \frac{|\kappa_1^2|}{s}\right] A(\beta_1, |\kappa_1^2|). \quad (3.9)$$

Within the double-log approximation we rewrite the (3.8) in terms of $\tilde{A} = \beta_1^{-1} A$ and approximate the splitting function $P^{(0)}(\beta)$ (3.5) by

$$P^{(0)}(\beta) \approx 2C_F \beta. \quad (3.10)$$

The resulting double-log equations read

$$\begin{aligned} \tilde{A}(\beta_1, |\kappa_1^2|) &= \frac{g^2 C_F}{(2\pi)^2} \int_{\beta_1}^1 \frac{d\beta_2}{\beta_2} \int_{\mu^2}^{|\kappa_1|^2 \beta_2 / \beta_1} \frac{d|\kappa_2^2|}{|\kappa_2^2|} \tilde{A}(\beta_2, |\kappa_2^2|) \\ &+ \tilde{A}_0(\beta_1, |\kappa_1^2|) \\ \tilde{A}_0(\beta_1, |\kappa_1^2|) &= \frac{g^2 C_F}{(2\pi)^2} \end{aligned} \quad (3.11)$$

and

$$\begin{aligned} h_1(x, Q^2) &= \int_{\mu^2/s}^1 d\beta_1 \beta_1 \int_{\mu^2}^{s/4} \frac{d|\kappa_1^2|}{|\kappa_1^2|} \\ &\cdot \delta\left[\beta_1 - x - \frac{|\kappa_1^2|}{s}\right] \tilde{A}(\beta_1, |\kappa_1^2|). \end{aligned} \quad (3.12)$$

Equation (3.11) is to be compared with the corresponding equation for the flavour non-singlet structure function $F_1(x, Q^2)$ [16]. The solution can be written in terms of a Bessel function $I_2(z)$ [20].

3.3 Separation of the smallest transverse momentum

The double-log contribution can also be treated by the method of separation of softest particle [15]. It leads directly to simpler equations in terms of partial waves with a quadratic term. A particular advantage of this approach is that both signature parts of the amplitude $A(s, \kappa^2)$ can be calculated in the double-log approximation

$$\begin{aligned} A(s, \kappa^2) &= A^+(s, \kappa^2) + A^-(s, \kappa^2) \\ A^\pm(s, \kappa^2) &= \int_{-i\infty}^{i\infty} \frac{d\omega}{2\pi i} \zeta^\pm(\omega) \left(\frac{s}{|\kappa^2|}\right)^{-1+\omega} f^\pm(\omega). \end{aligned} \quad (3.13)$$

Note that because this double-log contribution behaves like s^{-1} , the definition of the partial wave (3.13) differs in comparison with (2.14). For small ω the signature factor behaves like

$$\zeta^\sigma(\omega) \approx \begin{cases} -\frac{i\pi}{2} \omega & \sigma = +1 \\ 1 & \sigma = -1 \end{cases}. \quad (3.14)$$

There are two types of double-log contributions from loops with the smallest transverse momentum. The contribution of loops with a soft gluon of bremsstrahlung type is expressed in terms of the original amplitude with the gluon attached to the external lines. The contribution of

a two-particle intermediate state with the smallest κ is expressed in terms of a loop integral where the amplitude appears twice. The latter contribution results in a quadratic term in equations for $f^\pm(\omega)$. The double-log integration range established in (3.7) implies the existence of this contribution of the soft two-particle intermediate state in our case. In the previous subsection we summed in fact the double-log contributions of the latter type. The bremsstrahlung type contribution cancel in fact in the colour singlet channel of negative signature [15]. The integral equation (3.8) applies just to this case.

We need the result for the partial waves for colour singlet exchange. It is given in [15] (in our case $a_0 = 2C_F$ and the roles of positive and negative signatures are interchanged),

$$\begin{aligned} f_0^-(\omega) &= 4\pi^2 \omega \left(1 - \sqrt{1 - \frac{g^2 C_F}{\pi^2 \omega^2}} \right), \\ f_0^+(\omega) &= 4\pi^2 \omega \left(1 - \sqrt{1 - \frac{g^2 C_F}{\pi^2 \omega^2} \left(1 - \frac{1}{2\pi^2 \omega} f_0^-(\omega) \right)} \right). \end{aligned} \quad (3.15)$$

In (3.15), the positive signature partial wave $f_0^+(\omega)$ is expressed in terms of the negative signature partial wave of the colour octet channel $f_0^-(\omega)$ equal [15]

$$f_0^-(\omega) = 2g^2 N \frac{d}{d\omega} \ln \left\{ e^{\omega^2/4\bar{\omega}^2} \mathcal{D}_p \left(\frac{\omega}{\bar{\omega}} \right) \right\}, \quad \bar{\omega} = \left(\frac{g^2 N}{4\pi^2} \right)^{1/2} \quad (3.16)$$

where $\mathcal{D}_p(z)$ is the parabolic cylinder function [19] with $p = -1/2N^2$. Equation (3.15) implies that the leading Regge singularity for positive signature lies to the right of the negative signature singularity by a small amount

$$\omega_0^+ \approx \omega_0^- \left(1 + \frac{1}{2N^2} \right), \quad \omega_0^- = \left(\frac{g^2 C_F}{\pi^2} \right)^{1/2} \quad (3.17)$$

The partial waves (3.15) and (3.16) determine the Regge asymptotics of the scattering amplitude in the double-log approximation. In particular, the result (3.17) for the leading singularity ω_0^+ implies the existence of a contribution to $h_1(x, Q^2)$ with

$$h_1(x, Q^2)|_{\text{double-log}} \sim \left(\frac{1}{x} \right)^{-1 + \omega_0^+}. \quad (3.18)$$

The large Q^2 behaviour in the small x region can also be extracted from the partial waves (3.15) and (3.16). Indeed they determine the asymptotic anomalous dimensions $v(j)$ with the contributions proportional to $(g^2/(j+1)^2)^n$ summed to all orders n

$$v(j) = \frac{1}{8\pi^2} f_0^+(j+1), \quad \omega = j+1. \quad (3.19)$$

We checked that the first order term coincides with the leading term for $\omega \rightarrow 0$ of the moments calculated from the

one-loop splitting function (3.5)

$$v^{(1)}(j) = \frac{g^2}{8\pi^2} \int_0^1 dx x^{j-1} \cdot P^{(0)}(x) \Big|_{j \rightarrow -1} = \frac{g^2}{8\pi^2} \cdot \frac{2C_F}{j+1}. \quad (3.20)$$

4 Discussion

There are arguments in favour of the similarity of the transversity distribution $h_1(x, Q^2)$ and the helicity distribution $g_1(x, Q^2)$ at $x \rightarrow 1$ [5]. In particular the one-loop parton splitting function for the flavour non-singlet $g_1(x, Q^2)$ and for $h_1(x, Q^2)$ match at $x \rightarrow 1$.

Summarizing our results we have seen, however, that at small x the structure function $h_1(x, Q^2)$ behaves quite different from $g_1(x, Q^2)$. For $g_1(x, Q^2)$ the flavour singlet part leads to a rapid increase towards small x , and also the non-singlet part shows some increase [10].

Instead for $h_1(x, Q^2)$ at small x we have encountered two contributions.

The first contribution is roughly constant in x and shows also a weak Q^2 dependence. It results from the sum of the leading perturbative Regge contributions from the exchange of two reggeized fermions with opposite chirality. Contrary to the case of equal chirality they are of simple logarithmic type with the logarithm resulting from the longitudinal momentum integration in each loop. Adopting a model for the corresponding proton impact factor we have given a rather explicit form of this first contribution, (2.26).

The second contribution is non-leading compared to the first one at small x , (3.18). It arises as a sum of all contributions with leading logarithms both from longitudinal and transverse momentum integrations. It includes the small x asymptotics of GLAP evolution, which corresponds to restricting the transverse momentum integration range to the strongly ordered configurations. Since the double log range exceeds this strongly ordered one, the actual small x behaviour of this second contribution deviates from the GLAP behaviour in the same sense as in the flavour non-singlet $F_1(x, Q^2)$ or $g_1(x, Q^2)$ cases [16, 10] (see also [21]). Compared to the structure functions mentioned above it appears as an unusual feature here that the dominant contribution at small x does not include GLAP asymptotics. This fact makes the studies of $h_1(x, Q^2)$ in the region of x in which both contributions play a role very interesting.

We have concentrated on the contribution with positive signature. The leading lns asymptotics in the negative signature case is influenced by a three Reggeon exchange, for which no explicit results are known.

The results derived in this paper are obtained within the leading logarithm approximation and the double logarithmic approximation. Due to that we are unable to give prediction about the relative weight of two contributions mentioned above and to give an estimate at which value of x a deviation from GLAP evolution has to be expected.

Acknowledgements. A.Sch.'s and L.Sz.'s research was supported by the DFG grant (Sch 458/3). L.M.'s research was supported by BMBF and by KBN grant 2 P03B 065 10. R.K. and L.Sz. acknowledge the support of the German-Polish agreement on scientific and

technological cooperation N-115-95. L.Sz. would like to acknowledge the warm hospitality extended to him at J.W. Goethe Universität Frankfurt am Main.

References

1. Ralston and D.E. Soper, Nucl. Phys. B154 (1979) 109.
2. R.L. Jaffe and X. Ji, Phys. Rev. Lett. 67 (1991) 553; Nucl. Phys. B375 (1992) 527.
3. Proceedings of "Polarized Collider Workshop", University Park, PA 1990, Eds.: J. Collins, S.F. Heppelman and R.W. Robinet, Conference Proceedings No. 223, Particles and Fields Series 42, American Institute of Physics, New York 1991; Proceedings of "Workshop on the Prospects of Spin Physics at HERA", August 28-31, 1995, Zeuthen, Germany, Eds.: J. Blümlein and W.-D. Nowak, DESY 95-200.
4. R.L. Jaffe, "The context of high energy spin physics", Talk presented at the Adriatico Research Conference "Trends in Collider Spin Physics", ICTP, Trieste, Italy, 5-7 Dec. 1995, hep-ph/9603422.
5. R.L. Jaffe, "Spin, twist and hadron structure in deep-inelastic processes", Lecture at Erice School "The Spin Structure of the Nucleon", hep-ph/9602236.
6. X. Artru and M. Mekhfi, Zeit. f. Physik C45 (1990) 669.
7. A.P. Bukhvostov, G.V. Frolov, E.A. Kuraev and L. Lipatov, Nucl. Phys. B258 (1985) 601.
8. J.C. Collins, Nucl. Phys. B394 (1993) 169.
9. B.L. Ioffe and A. Khodjamirian, Phys. Rev. D51 (1995) 3373.
10. Bartels, B.I. Ermolaev and M.G. Ryskin, DESY preprints DESY-05-124 hep-ph/9507271 and DESY 96-025 hep-ph/9603204.
11. Ya.I. Asimov, ZhETF 43 (1962) 2321; S. Mandelstam, Nuovo Cim. 30 (1963) 1127; V.N. Gribov, I.Ja. Pomeranchuk and K.A. Ter-Martirosyan, Yad. Fiz. 2 (1965) 361.
12. V.N. Gribov and L.N. Lipatov, Sov. J. Nucl. Phys. 15 (1971) 78; L.N. Lipatov, Sov. J. Nucl. Phys. 20 (1974) 94; G. Altarelli and G. Parisi, Nucl. Phys. B126 (1977) 298.
13. L.N. Lipatov, Sov. J. Nucl. Phys. 23 (1976) 642; V.S. Fadin, E.A. Kuraev and L.N. Lipatov, Phys. Lett. 60B (1975) 50; Sov. Phys. JETP 44 (1976) 443; *ibid* 45 (1977) 199; Y.Y. Balitski and L.N. Lipatov, Sov. J. Nucl. Phys. 28 (1978) 882.
14. R. Kirschner, L. Lipatov and L. Szymanowski, Nucl. Phys. B425 (1994) 579; Phys. Rev. D51 (1995) 838.
15. R. Kirschner and L. Lipatov, ZhETF 83 (1982) 488; Nucl. Phys. B213 (1983) 122.
16. B.I. Ermolaev, S.I. Manayenkov and M.G. Ryskin, Zeit. f. Phys. C69 (1996) 259.
17. V.S. Fadin and V.E. Sherman, Sov. Phys. JETP 45 (1977) 861.
18. R. Kirschner, Zeit. f. Physik C67 (1995) 459; *ibid* C65(1995) 505.
19. I.S. Gradstein and I.M. Ryshik, "Tables of series, products and integrals", MIR, Moscow 1981.
20. V.N. Gribov, V.G. Gorshkov, G.V. Frolov and L.N. Lipatov, Sov. J. Nucl. Phys. 6 (1967) 95; V.G. Gorshkov, Sov. Phys. Uspekhi 16(1973) 322.
21. Blümlein and A. Vogt, Phys. Lett. B370(1996) 149.